IEEE Access
Multidisciplinary | Rapid Review | Open Access Journal

Received February 4, 2019, accepted February 18, 2019, date of publication March 1, 2019, date of current version March 25, 2019.

Digital Object Identifier 10.1109/ACCESS.2019.2902242

Vertical Wind Profile Characterization and Identification of Patterns Based on a Shape Clustering Algorithm

ANGEL MOLINA-GARCÍA[1], (Senior Member, IEEE), ANA FERNÁNDEZ-GUILLAMÓN[1], EMILIO GÓMEZ-LÁZARO[2], (Senior Member, IEEE), ANDRÉS HONRUBIA-ESCRIBANO[2], AND MARÍA C. BUESO[3]

[1]Department of Electrical Engineering, Universidad Politécnica de Cartagena, 30202 Cartagena, Spain
[2]Renewable Energy Research Institute, DIEEAC, EDII-AB, Universidad de Castilla-La Mancha, 02071 Albacete, Spain
[3]Department of Applied Mathematics and Statistics, Universidad Politécnica de Cartagena, 30202 Cartagena, Spain

Corresponding author: Angel Molina-García (angel.molina@upct.es)

This work was supported in part by the Spanish Ministry of the Economy and Competitiveness and the European Union under Grant ENE2016-78214-C2-2-R, and in part by the Spanish Education, Culture and Sport Ministry under Grant FPU16/04282.

ABSTRACT Wind power plants are becoming a generally accepted resource in the generation mix of many utilities. At the same time, the size and the power rating of individual wind turbines have increased considerably. Under these circumstances, the sector is increasingly demanding an accurate characterization of vertical wind speed profiles to estimate properly the incoming wind speed at the rotor swept area and, consequently, assess the potential for a wind power plant site. This paper describes a shape-based clustering characterization and visualization of real vertical wind speed data. The proposed solution allows us to identify the most likely vertical wind speed patterns for a specific location based on real wind speed measurements. Moreover, this clustering approach also provides characterization and classification of such vertical wind profiles. This solution is highly suitable for a large amount of data collected by remote sensing equipment, where wind speed values at different heights within the rotor swept area are available for subsequent analysis. The methodology is based on z-normalization, shape-based distance metric solution, and the Ward-hierarchical clustering method. Real vertical wind speed profile data corresponding to a Spanish wind power plant and collected by using commercial Windcube equipment during several months are used to assess the proposed characterization and clustering process, involving more than 100 000 wind speed data values. All analyses have been implemented using open-source R-software. From the results, at least four different vertical wind speed patterns are identified to characterize properly over 90% of the collected wind speed data along the day. Therefore, alternative analytical function criteria should be subsequently proposed for vertical wind speed characterization purposes.

INDEX TERMS Clustering algorithms, patterns clustering, wind power generation.

I. INTRODUCTION

Most developed countries are now promoting large-scale integration of Renewable Energy Sources into power systems [1]. Among these renewables, wind power is considered the most efficient and developed energy source [2]. Indeed, it is expected that 323 GW of wind energy capacity will be installed in Europe by 2030, covering more than 30% of the electricity demand [3]. In fact, during recent decades, current wind turbine size has evolved from less than 100 kW to 3500 kW [4]. Full converter wind turbines can provide greater flexibility and energy efficiency, convering power ratings between 4.5 MW and 7 MW [5]. At the same time, the increase in both the hub height and the area swept by the blades has drawn interest to better understanding the structure of the vertical profile of the horizontal wind [6]. Furthermore, since the power extracted by a wind turbine is highly dependent on the wind speed, an accurate estimation of vertical wind speed profiles v_H (the horizontal wind speed at height H) is required by the sector [7]. To determine

The associate editor coordinating the review of this manuscript and approving it for publication was Qilian Liang.

the horizontal wind speed at hub height, two methods have been widely used in the wind sector: (*i*) direct methods and (*ii*) indirect methods.

Direct methods are implemented by installing meteorological towers equipped with conventional wind speed meters at a suitable height or, more recently, by remote sensing such as SoDAR (Sonic Detection And Ranging) or LiDAR (Light Detection and Ranging) systems. The most commonly used speed meters are based on anemometers and windmills. Cup anemometers are formed by three or four cups equidistant from each other and coupled to a vertical rotational axis. Windmills are usually composed by four blades. Both anemometers and windmills have an error of around ±2%, and collect horizontal wind speed values at only one height. Therefore, it should be required to estimate other wind speed values at the rotor swept area. SoDAR and LiDAR are based on the Doppler effect, receiving the reflection of sound and light, respectively. Apart from their significant accuracy (98% for SoDAR and 99.6% for LiDAR), they can collect wind speed data at different heights without needing a meteorological tower [8], which is an important advantage in comparison to the previous solutions. Moreover, LiDARs can also be used to obtain three-dimensional wind measurements [9]. Several studies can be found in the specific literature comparing these techniques or addressing different assessment analysis [10]. A comparison between LiDAR and cup anemometers was performed in [11], obtaining a high availability of 98% at the hub height in line with previous contributions [12]. A particular study in the Arctic middle atmosphere is described in [13], where mean wind speed values from LiDAR observations are compared to two different databases (ECMWF and HWM07). The results show that below $h \leq 55$ km the differences are smaller than 2 – 5 m/s. Recent contributions focused on optimizing LiDAR for wind turbine control can be found in [14] and [15]. Regarding SoDAR solutions, suggested in [16], they can present root-mean-square errors of around 2% compared to mast-mounted cup anemometers. In [17], the results between SoDAR and the cup anemometer show some differences mainly due to the measurement field campaigns, which were conducted in different locations. A comparison between LiDAR, SoDAR and mast-mounted cup anemometer was carried out in [18]. Although a successful correlation level was found, both LiDAR and SoDAR collected lower wind speed values than the cup anemometers. According to [19], the SoDAR is highly dependent on temperature variation in the atmosphere, which is a substantial drawback compared to LiDAR solutions. However, a cost analysis reveals that SoDAR equipment is cheaper than the LiDAR [17].

Indirect wind speed estimation methods consist of measuring horizontal wind speed at a lower height and applying an extrapolation model to estimate the vertical wind speed profile. The most commonly used models are the power law, see (1), and the logarithmic law, see (2), [20].

$$v_H = v_{ref} \cdot \left(\frac{H}{H_{ref}}\right)^{\alpha} \tag{1}$$

$$v_H = \frac{u_*}{k} \cdot ln\left(\frac{H}{z_0}\right), \tag{2}$$

where v_H is the horizontal wind speed at height H, v_{ref} the horizontal wind speed at the reference height H_{ref}, α the Hellmann's exponent depending on roughness of the underlying terrain, u_* the surface friction velocity, k the von Karman's constant and z_0 the surface roughness length. These approaches present substantial drawbacks, since parameters such as α and z_0 may vary significantly according to the year, month, hour of the day, or depending on wind direction and speed values. In this sense, Gualtieri and Secci [21] discuss the diurnal variation of α and the monthly variation of z_0 for three different locations in Italy. Recent empirical equations derived by applying the power law to the relationship between the increase of wind speed and fetch lengths at 1–5 km con be found in [22]. An alternative function is known as the Deaves and Harris model (D–H model), see (3). This solution proposes a more realistic and complex expression to consider the atmospheric boundary layer physics [23],

$$v_H = \frac{u_*}{k}\left[ln\left(\frac{H}{z_0}\right) + 5.75\left(\frac{H}{h}\right) - 1.88\left(\frac{H}{h}\right)^2 - 1.33\left(\frac{H}{h}\right)^3 + 0.25\left(\frac{H}{h}\right)^4\right] \tag{3}$$

$$h = \left(\frac{u_*}{B \cdot f}\right), \tag{4}$$

where v_H, u_*, k and z_0 are the same parameters as in (2), h is the equilibrium boundary layer height, determined from (4), f is the Coriolis parameter and $B = 6$ an empirical constant estimated from observed wind speed profiles [24].

A comparison between the D-H model and the power law based on real collected data is discussed in [25]. From the results, the authors affirm that the suitability of the selected model is highly dependent on atmospheric conditions: unstable, neutral or stable. A comparison between collected vertical wind speed profiles and these three indirect models was conducted in [26]. In this case, the averaged real wind speed profiles agree with the D-H and the logarithmic models below 200 and 100 m respectively. However, no similarities were found between the power law approach and the measured profiles. A similar study was performed in [27], where the D-H model provided the best estimations in comparison with measured data. Recently, new models have been proposed in the specific literature. In [28], a neuro-fuzzy model is provided to estimate vertical wind profiles up to 100 m by using measurements at 10, 20, 30 and 40 m. A method based on Wind Atlas Analysis and Application Program (WAsP) to improve vertical wind speed estimations by least squares (LES) methodology is described in [29]. Two different proposals using artificial neural network are described in [30], estimating vertical wind speed values up to 100 m from measures at 10, 20 and 30 m. A time series model of wind speed for day ahead forecasting is developed in [31], based on linear and nonlinear autoregressive models

TABLE 1. Review of previous studies.

Ref.	Methodology used	Year
[13]	Comparison between LiDAR and two databases (ECMWF and HWM07)	2017
[17]	Comparison between SoDAR and cup anemometer	2017
[21]	Power law applied to anemometer measurements	2011
[25]	Comparison between D-H model and power law	2017
[32]	Revised power-law model	2018
[26]	Anemometers at different heights	2010
[27]	Comparison between LiDAR and data collected in a nearby place	2013
[28]	Adaptive neuro-fuzzy method	2011
[30]	Artificial neural network	2017
[33]	Comparison between power law, logarithmic law and real data	2015
[34]	Power law for low speed conditions (prevailing air and thermal pollution)	2017

with and without exogenous variables. A review of methodologies used in some of the previously mentioned studies is summarized in Table 1.

According to the specific literature, most contributions are thus focused on proposing different expressions to estimate vertical wind speed profiles from data provided by anemometers. Indeed, it is very common their application in the wind energy sector along the decades [35]–[37]. However, and assuming the power density (PD) —defined as the ratio between rated power output and rotor's swept area (in W/m^2)— as a relevant indicator of the power wind turbine [38], several studies conclude that the wind speed at hub height is not representative for the whole area. Moreover, it leads to inconsistencies in power curve measurements for large wind turbine [39]. For this reason, recent works affirm that it is preferable to take measures at two or three levels, for one period at least six months [40]. Post processing methods should be then applied on these collected raw data to extract explanatory information of most likely vertical wind speed profiles. Under this scenario, there is a lack of contributions devoted to characterizing a large amount of real wind speed data. Moreover, solutions to identify common vertical wind speed patterns and, consequently, make both representation and characterization easier are more and more required by the sector to analyze a location and the corresponding vertical wind resource in detail. Therefore, a characterization of raw wind power data is needed to estimate properly the wind power capable to produce energy and subsequently to allow us new proposals of vertical wind speed profile modeling, since nowadays there is no uniform analytic expression valid for all wind stability conditions [41]. The main contributions of this paper are then summarized as follows:

- A novel wind speed analysis to identify vertical wind speed patterns from a large amount of collected wind speed data is proposed and assessed.
- A shape-based clustering analysis is evaluated to provide most likely vertical wind speed patterns along the day based on real wind speed data collected with a LiDAR system.
- The proposed solution, implemented in the open-source *R*-software with unrelevant computational time cost, can be adapted to different locations from the corresponding raw data and the field-measurement campaigns.

This work is in line with previous contributions by the authors, where the aggregated wind power generation was characterized based on Weibull mixtures [42]. The rest of the paper is organized as follows: Section II discusses the time-series clustering techniques used to characterize wind speed profiles; Section III describes the proposed methodology; the results are described and discussed in Section IV; and, finally, the conclusions are presented in Section V.

II. FUNCTIONAL CLUSTERING: BACKGROUND AND RELATED WORK

A. GENERAL OVERVIEW

Clustering is one of the most commonly used data mining techniques to find homogeneous subgroups of entities depicted in a set of data [43], [44]. A cluster analysis involves sorting data objects into groupings (labeled as clusters) based on similarity [45]. Although the notion of *'cluster'* is not unique [46], the global goal is that the objects of a group are similar to one another and different from the ones in other groups [47]. According to [48], various clustering algorithms can be found in the specific literature:

- *Hierarchical methods:* Clusters are determined by recursively partitioning the instances. There are two types: agglomerative hierarchical clustering (objects are considered as clusters that are merged successively) and divisive hierarchical clustering (all objects belong to one cluster that is divided successively into sub-clusters).
- *Partitioning methods:* The objects are relocated by moving them from one cluster to another, starting from an initial partitioning. There are two methods: error minimization algorithms —these find a clustering structure that minimizes a certain error criterion. This measures the 'distance' of each object to its representative value— and graph-theoretic clustering —determining clusters via graphs—.
- *Density-based methods:* It is assumed that the points that belong to each cluster are drawn from a specific probability distribution.
- *Model-based clustering methods:* Optimizing the fit between given data and some mathematical models.

A large number of functional clustering applications can been found in the literature review [49], mainly focused on life sciences [50]. Nevertheless, a number of authors have proposed the use of functional clustering approaches for power system purposes. A comparison of various unsupervised clustering algorithms to group customers with similar electrical behavior is provided in [51]. In [52], a functional clustering procedure is used to classify the daily power load curves of four separated periods, providing a short-term peak load forecasting methodology. A clustering methodology able to improve short-term functional time series forecasts of household-level electricity demand is presented

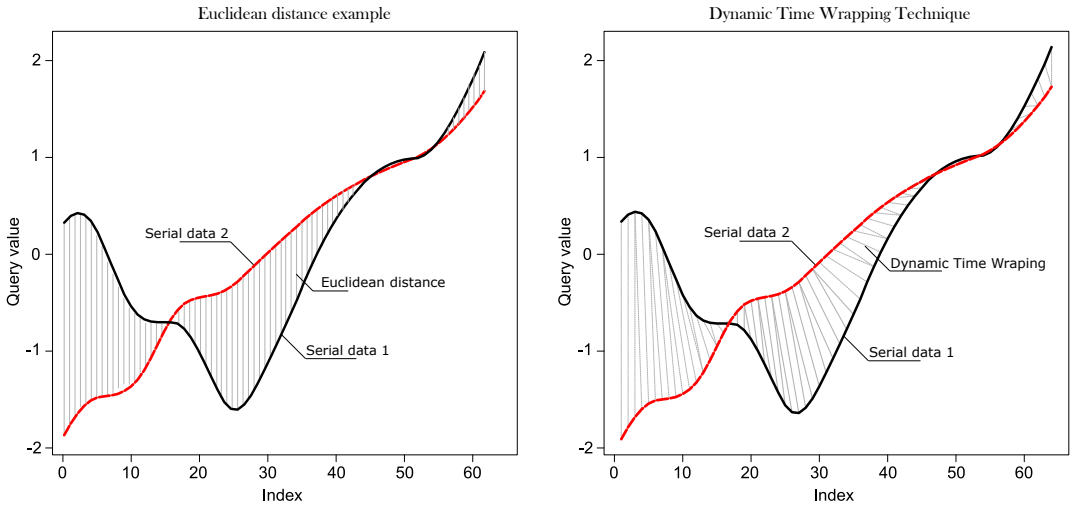

FIGURE 1. Dynamic Time Warping (DTW) technique example.

in [53]. A forecasting model for day-ahead and hour-ahead load predictions is developed in [54] based on artificial neural networks and clustering. A novel clustering-based fuzzy wavelet neural network model is also proposed in [55]. Data mining techniques have been also proposed to analyze SCADA measurements collected on onshore wind power plants, but focused on power curve analysis [56]. In our specific study, and taking into account the efficiency issue of hierarchical clustering, which can be applied to most types of data [57], the agglomerative hierarchical clustering is selected. This approach usually involves higher computational time costs than partitional clustering, but requires non-predefined parameters [58]. Specifically, Ward's hierarchical clustering method is used to estimate the different clusters, which is carried out in a multivariate Euclidean space [59].

B. DISSIMILARITY MEASURES

With regard the time-series clustering, different algorithms have been developed in the specific literature considering a wide set of dissimilarity or distance measures [60]. One of the most popular and field-tested similarity measures is the Dynamic Time Warping (DTW) distance, based on the optimum warping path between time-series [61]. DTW has been widely used in many areas and is a popular automatic speech recognition (ASR) method [62]. Indeed, it is a flexible and much more robust distance measure, allowing similar shapes to be matched even if they are out of the phase in the time axis [63]. Given two discrete time-series $X = (x_1, x_2, \ldots, x_n)$ and $Y = (y_1, y_2, \ldots, y_m)$ with $n, m \in \mathbb{N}$, we define the cross-distance matrix ($M \in \mathbb{R}^{n,m}$) as follows:

$$m_{ij} = d(i,j) = f(x_i, y_j) \geq 0. \tag{5}$$

The most common choice is to assume the Euclidean distance $m_{ij} = d(i,j) = (x_i - y_j)^2$. The algorithm then finds the alignment path through the low-cost areas of the cross-distance matrix. It is typically subjected to the following constraints: boundary conditions, continuity and monotonicity [64]. A warping path that minimizes the distance between both time-series can then be estimated by [65]:

$$DTW(X,Y) = min\left[\sum_{k=1}^{K} m_{kk} = d(k,k) = f(x_k, y_k)\right], \tag{6}$$

where $max(n,m) \leq K \leq m + n + 1$. Further information and some examples of DTW technique can be found in [66]–[68]. In addition, Fig. 1 shows an example of the DTW technique application and a comparison to the Euclidean distance approach for two random trajectories. The *dtw*–function is applied by using the `dtw` *R*–software package [69].

DTW approach can also be extended to measure the similarity between two N-dimensional sequences [70]. An example of a multi-dimensional Dynamic Time Warping (msDTW) approach can be found in [71]. According to some authors, and assuming that DTW is a major solution in the field of time series classification problem, it has quadratic space and time complexity that might lead to memory problems under long time series data [72]. As a faster alternative to the DTW algorithm, the Shape-Based Distance (SBD) metric was proposed by Paparrizos and Gravano [68]. It is based on coefficient-normalized cross-correlation. It is used in the present work as an improved methodology of DTW metric solutions. To provide scale invariance and remove inherent distortion in the collected data, we implement the z-normalization of the horizontal wind speed values. This z-normalization is based on the standard (0, 1) statistical normalization: vectors are linearly transformed by subtracting their feature means and dividing by their standard-deviations [73],

$$z_i = \frac{x_i - \mu_X}{\sigma_X}, \tag{7}$$

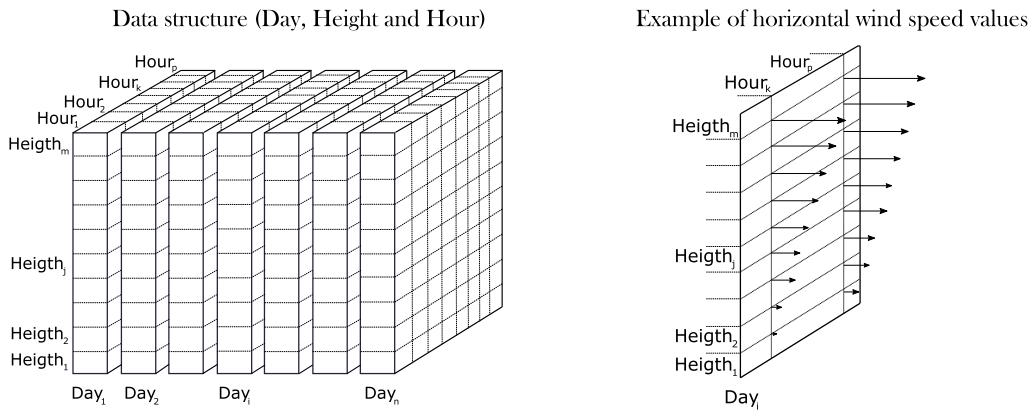

FIGURE 2. General data scheme and example of horizontal wind speed data. General overview.

All analyses have been conducted using open-source R-software [74]. The `dtwclust` *R*-package is used for the SBD metric estimation [75].

III. METHODOLOGY

Taking into account both the SBD algorithm and Ward's hierarchical clustering method previously discussed in Section II, a characterization methodology to identify wind speed profile patterns and visualize most common tendencies is now described in detail. This approach allows us to characterize large amounts of wind speed data collected in real locations by means of clustering and pattern identification. The solution is thus highly suitable for data collected by remote sensing equipment, where wind speed values at different heights are available to be analyzed. Fig. 2 shows schematically the data structure and an example of horizontal wind speed data for the different heights and by considering a specific day (Day_i) and hour (Hour_k).

The proposed methodology is firstly based on a filtering real data stage. With this aim, a preliminary data analysis was carried out to remove non-expected and/or wrong data. Subsequently, wind speed curves with missing data or more than 50% of the wind speed values below 4 m/s were not considered. Most wind turbines currently have a minimum starting wind speed range over 4 m/s. Recent contributions focused on dynamic data filtering for LiDAR wind speed measurements can be found in [76]. After this initial filtering process, and based on previous studies from collected data on on-shore Spanish wind power plants, it was detected that some of the $v - H$ curves were discordant. Indeed, it was even found that some of them were not functions at all, having two or more H values for just one v. To solve this problem, the author propose an axis rotation. $H - v$ curves are thus obtained, solving aforementioned the problem. It is worth noting that this drawback, mainly related to real data collected at different heights in on-shore wind power plants, has not been widely discussed in the specific literature, being neglected by most previous contributions. The filtered wind speed data are then fulfilled by using the *aspline* function with the objective of defining a unique and homogeneous height interval: from 40 to 160 m. Fig. 3 shows examples of wind speed collected data and their corresponding filtered and fulfilled values by the *aspline* function. Real data were collected for three months at a Spanish wind power plant located in the southeast of Spain. The wind speed data collected at different hours are summarized in the figure.

From these homogeneous groups of wind speed profiles, an interpolation process is then applied on a common grid, providing a positive power length of 2. In our case, a total of 512 points are estimated, being a 2 potential (2^9). The `Akima` R-software package is used for this interpolation process. Further information about this package can be found in [77]. Fig. 4 describes schematically the proposed axis rotational and spline process and the corresponding interpolated vertical wind speed profiles.

As was previously discussed in Section II, and aiming to provide scale invariance and remove inherent distortion in the data, a z-normalization process is applied to the spline values. Each wind speed curve is linearly transformed by subtracting their feature means and dividing by their standard-deviations. Fig. 5 shows an example of z-normalization process from real wind speed data previously filtered and splined. The SBD metric is then applied on the z-normalized data, providing an estimation of distances between the wind speed curves. These curves are divided into different hours of the day and, subsequently, distances among these curves correspond to those curves collected within the same hour. Finally, Ward's hierarchical clustering method was applied to estimate the most likely wind speed profile patterns for each time interval. Fig. 6 describes schematically the wind speed data structure and the selection process for a specific hour (Hour_k). The clustering application usually involves a visual inspection of the clustering in terms of deciding the optimal number of clusters. Other approaches propose different decision criteria for the optimal cluster number [78]. In our opinion, this optimal number of clusters is outside the scope of the present contribution and subsequently, the optimal number of clusters is then considered as a user-decision. From the corresponding wind speed patterns, a suitable and summarized

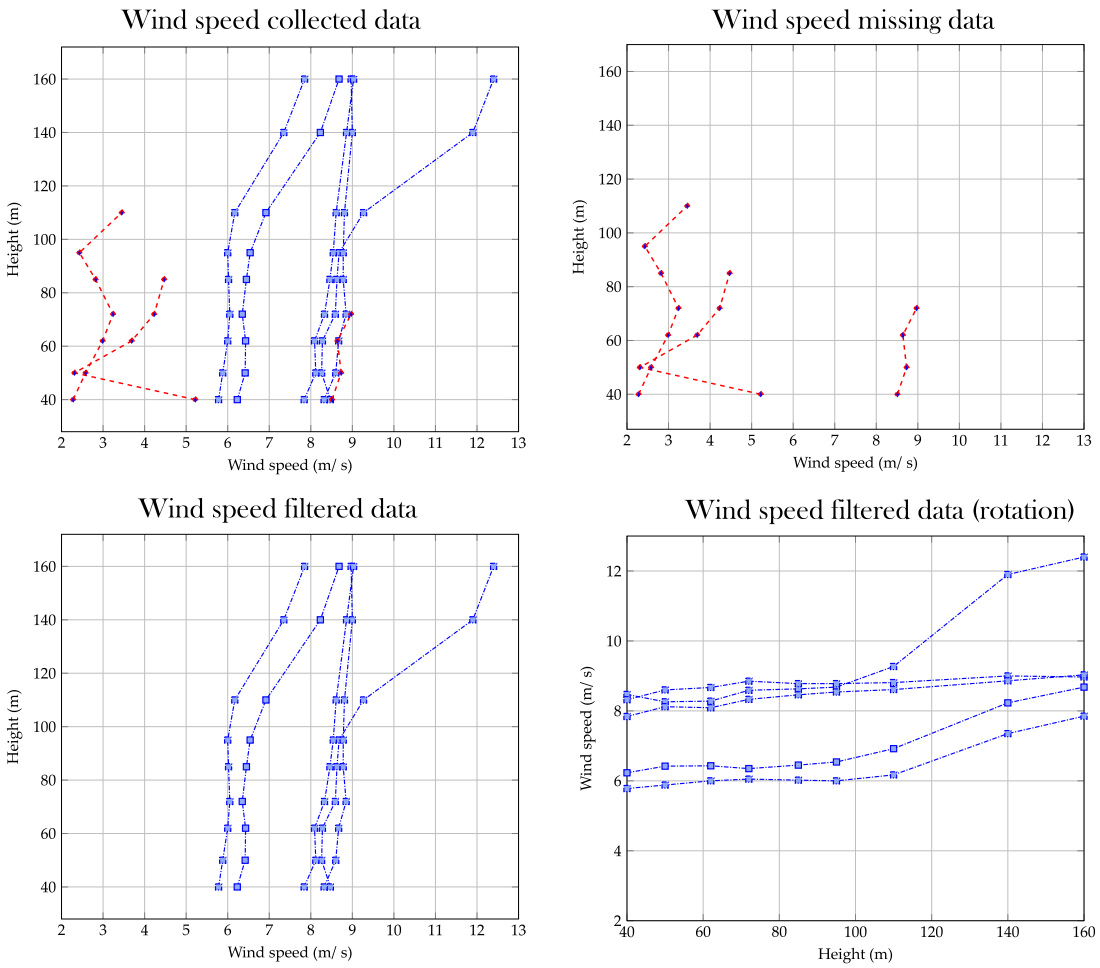

FIGURE 3. Example of filtering process application (Spanish Wind Power Plant).

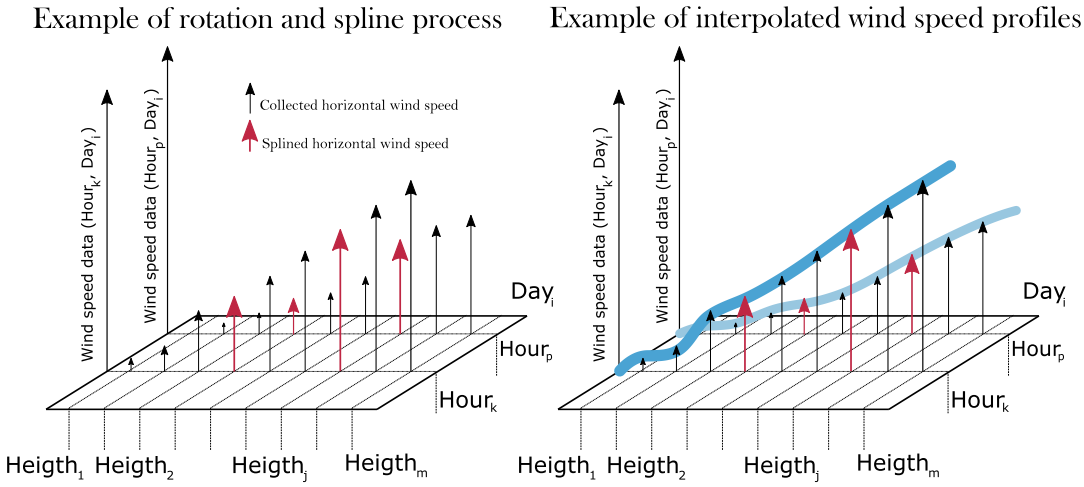

FIGURE 4. Axis rotational, spline data process and interpolated vertical wind speed profiles. General overview.

visualization of a large amount of real collected data through a reduced number of profiles is then provided. Indeed, these wind speed patterns give an accurate and precise preliminary analysis about the possibilities of proposing different analytical functions to characterize real wind speed curves. Moreover, the proposed visualization and characterization solution of real data also provides additional information to study collected data in detail and characterize the available

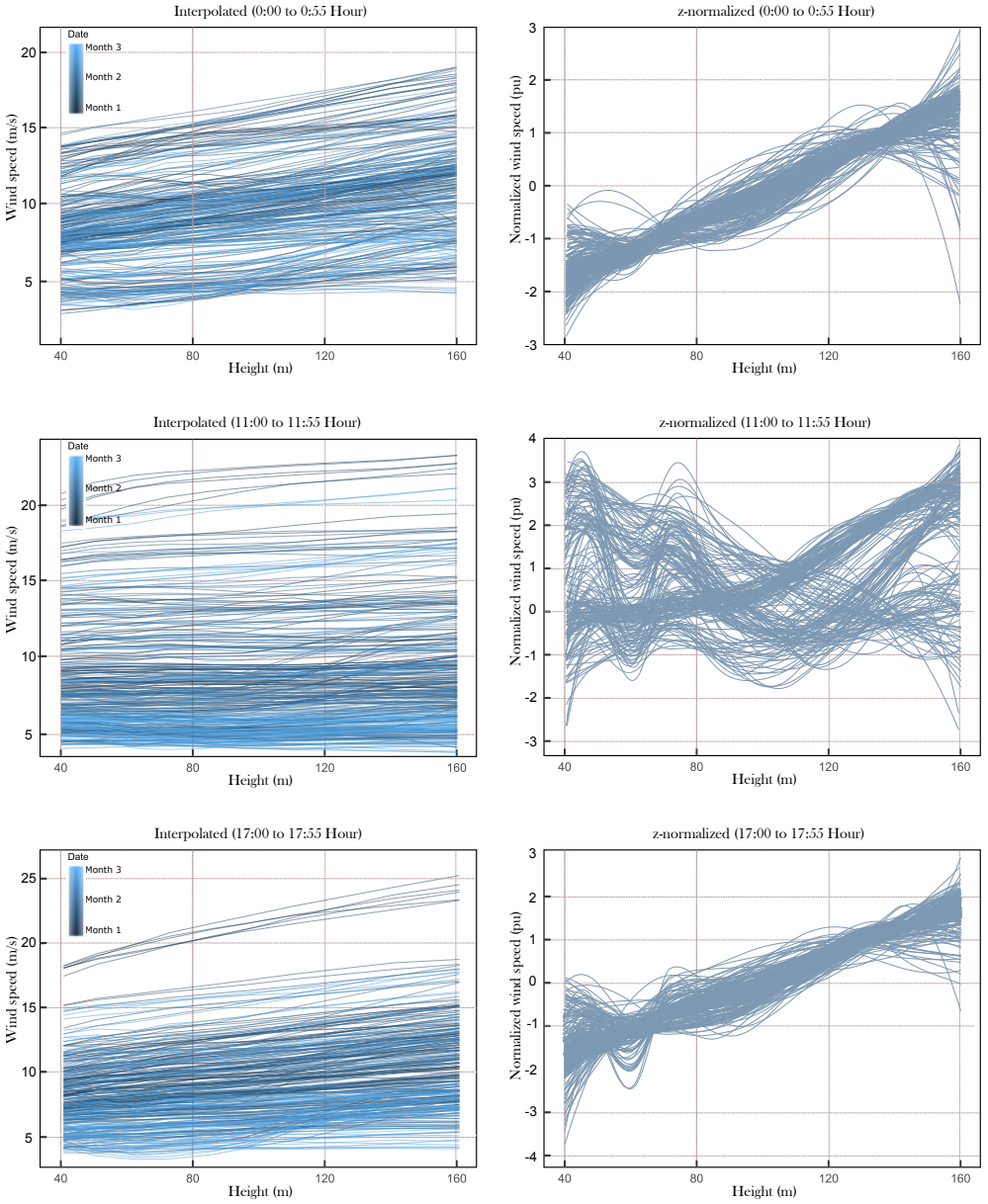

FIGURE 5. Example of interpolation and *z*-normalization process (Spanish Wind Power Plant).

wind resource. Fig. 7 summarizes the methodology proposed in this work.

IV. RESULTS

A. PRELIMINARIES

Wind speed data were collected at two Spanish wind power plants connected to the grid and located in the south of Spain. Different field measurement campaigns were carried out by using LiDAR equipment. More specifically, a commercial *WindCube* was installed in these locations to collect wind speed data over three months. Fig. 8 shows the equipment used for the field measurement campaigns. Wind speed curves were measured and collected with a 10 minute sample time interval. The height range of measurements was from 40 m to 200 m. Nevertheless, and with the aim of maximizing the number of data used for clustering purposes, wind speed heights were limited from 40 to 160 m since a significant amount of data at 200 m corresponded to wrong values or not-a-number values, as was mentioned in Section III. A total amount of 110230 data were initially analyzed. After the filtering process, a total wind speed values of 61551 were selected, corresponding to 6839 vertical wind speed profiles. By considering this initial group of vertical wind speed values, a subsequent characterization process is thus required by the sector to visualize the most likely vertical wind speed patterns.

Fig. 9 shows an example of the wind speed variability for a specific wind power plant and location, taking into account both maximum and minimum wind speed values based on the collected data at different heights —40, 52, 62, 72, 85,

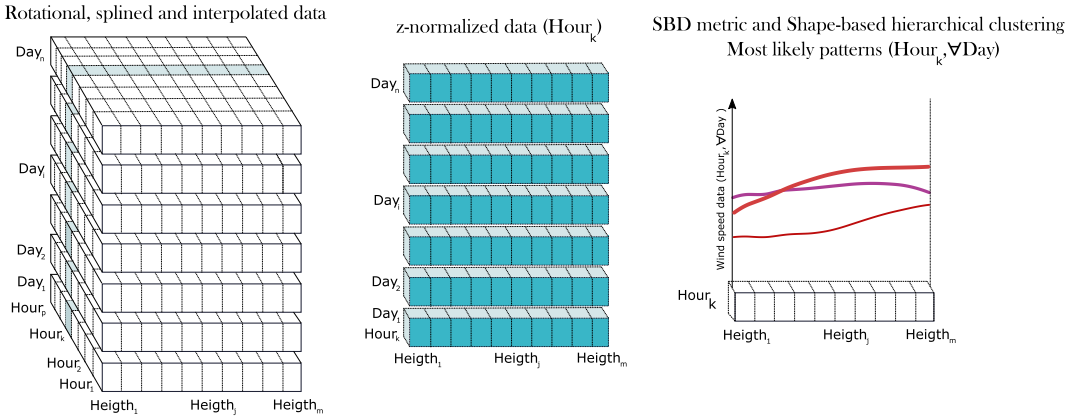

FIGURE 6. *z*-normalized, SBD metric and clustering process. General overview.

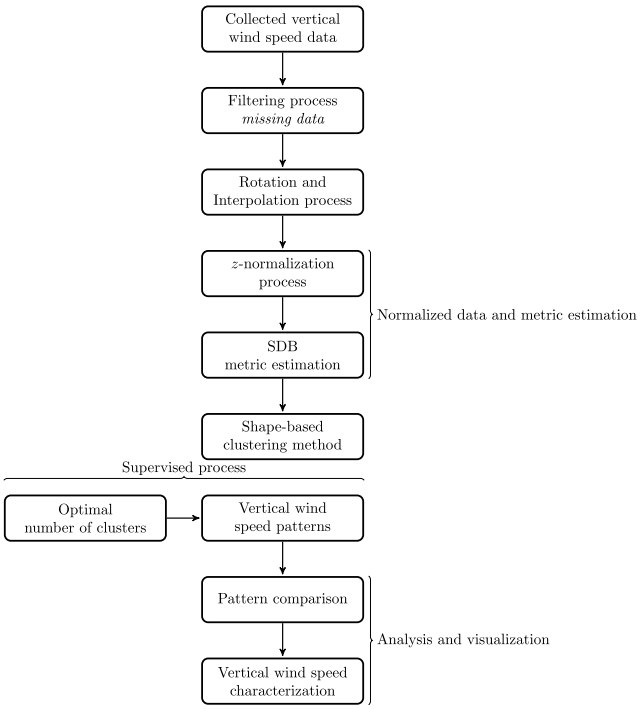

FIGURE 7. Proposed clustering and analysis methodology.

FIGURE 8. WindCurbe LiDAR equipment: example of field-test campaign (Albacete, Spain).

95, 110, 140 and 160 m—. As can be seen, there are relevant oscillations within the same hour for each day. Wind speed data are then *z*-normalized to estimate their corresponding wind speed curve patterns for each hour. Subsequently, a clustering process is applied on each hour to determine the most likely patterns throughout the day for the different hours.

B. FUNCTIONAL CLUSTERING CHARACTERIZATION. ANALYSIS

From the *z*-normalized wind speed data, and after dividing into different hours throughout the day, the SBD metric solution was applied to determine distances between splined vertical wind speed curves. According to the proposed methodology and as was previously discussed, the Ward's hierarchical clustering method involves a visual inspection of the results to determine a suitable number of clusters. Note that hirarchical clustering results are graphically represented on dengrograms. Fig. 10 depicts some dendrogram examples for different hours. Under these results, the number of 9 clusters was selected since it was considered suitable by the authors in order to characterize vertical wind speed profile variability across the different hours. Further information about a semi-supervised hierarchical clustering framework based on ultra-metric dendrogram distance can be found in [79].

Assuming a number of 9 clusters as a suitable classification of the different vertical wind speed groups for each hour, Fig. 11 summarizes the percentage of vertical wind speed profiles belonging to each cluster as a function of the hour of the day. As can be seen, night-time hours can be characterized by a lower amount of clusters in comparison

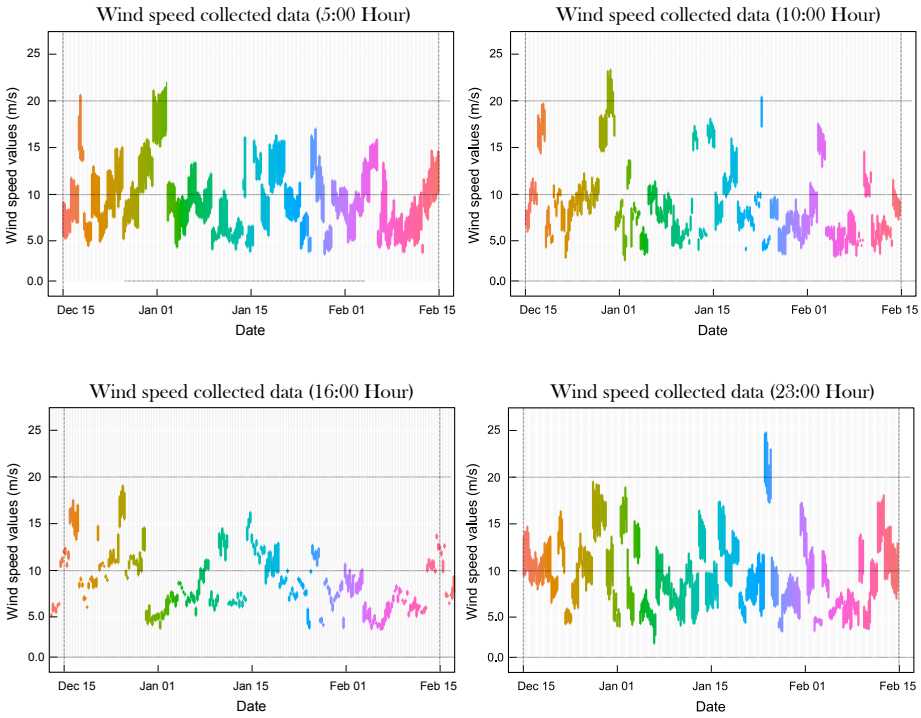

FIGURE 9. Example of wind speed data for a field measurement campaign (Collected data at different hours, Wind power plant located in Albacete, Spain).

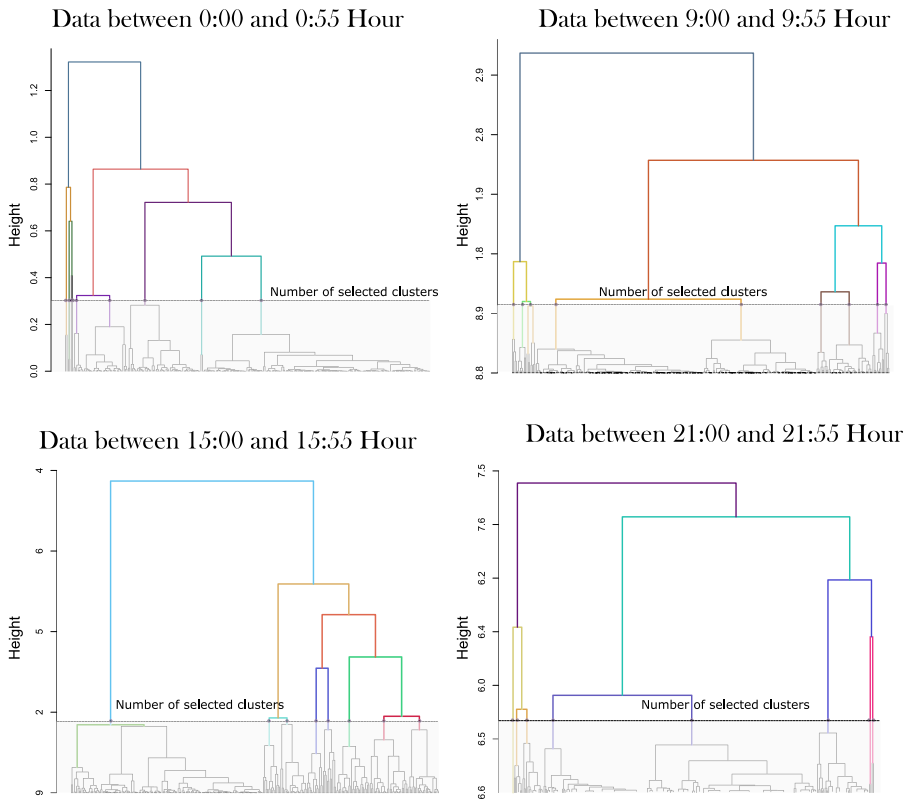

FIGURE 10. An illustrative examples of hirarchical clustering dendrograms.

to daylight hours. Indeed, 3 clusters accounts for over 75% of the vertical wind speed profiles for the night-time hours. However, daylight hours require a higher number of clusters to be characterized properly. As an example, 5 clusters are needed to account for 75% of the vertical wind speed data between 12:00 and 12:55 Hour. These results are in

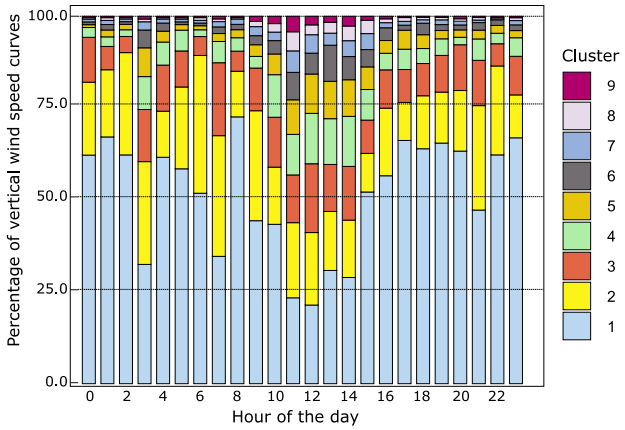

FIGURE 11. Cluster distribution per hours. Ward's hierarchical clustering process.

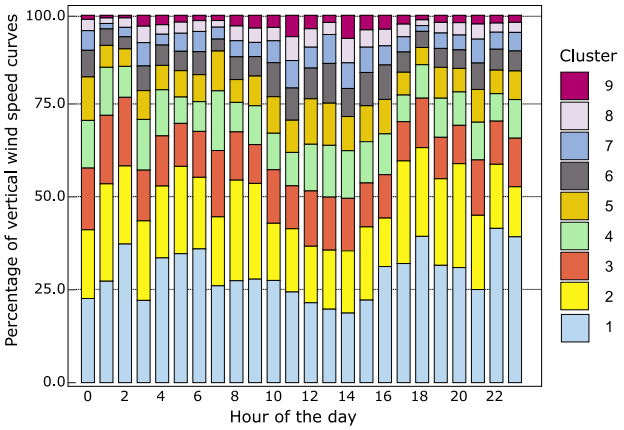

FIGURE 12. Cluster distribution per hours. Partitional clustering process.

line with other clustering techniques, such as partitional process. Aiming to compare both approaches Fig. 12 shows the percentages wind speed profiles, corresponding to the different clusters for each hour, when partitional clustering process is applied on the collected data. According to both methodologies, different vertical wind speed patterns are thus required to characterize the collected data, presenting a relevant heterogeneity in the vertical wind speed profiles. The rest of our analysis is conducted according to the Ward's hierarchical clustering results, by considering the distribution of the wind speed curves in the corresponding groups, as was depicted in Fig. 11.

Fig. 13 summarizes the classification of the collected vertical wind speed profiles according to the different clusters for data gathered between 4:00 and 4:55 Hour. In addition,

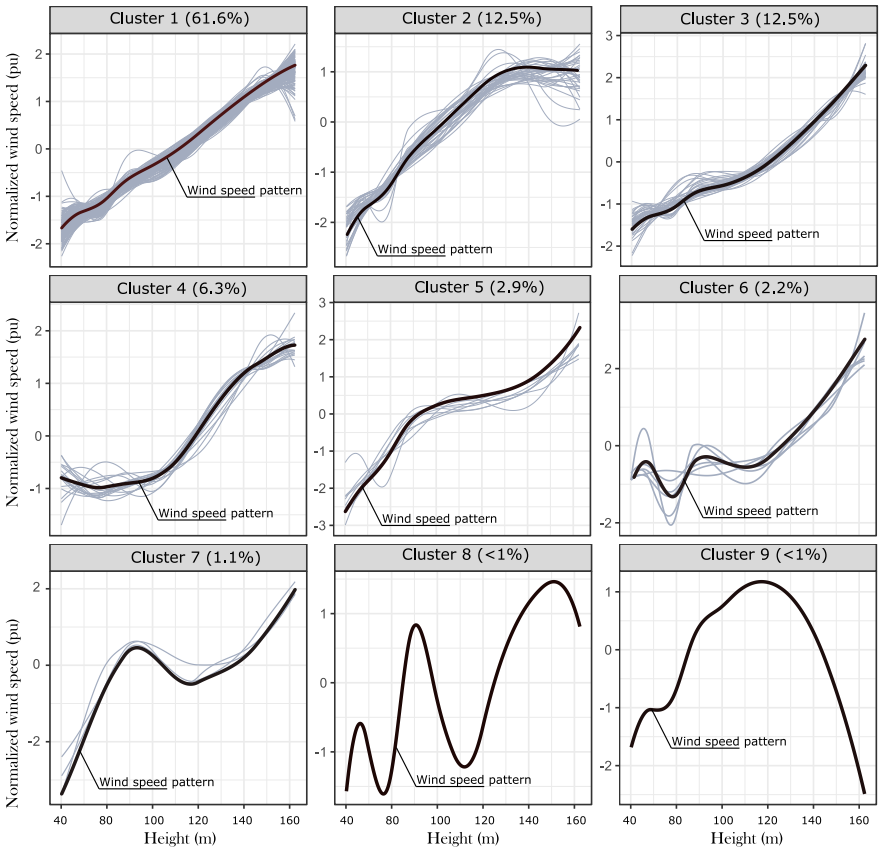

FIGURE 13. Example of *z*-normalized vertical wind speed distributed profiles (from 4:00 to 4:55 Hour). Ward's hierarchical clustering process.

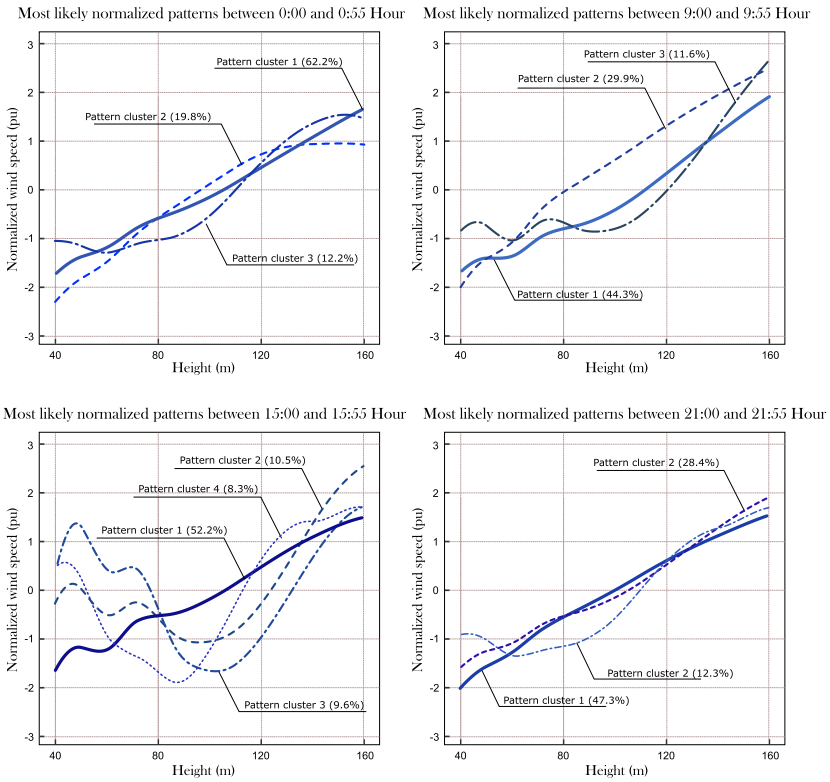

FIGURE 14. Examples of the most likely vertical wind speed normalized patterns. Results corresponding to several hours.

the vertical wind speed patterns are also included in the figure, as well as the percentage of curves corresponding to each cluster. As can be seen, clusters from 1 to 3 account for 86.6% of the collected wind speed curves. Therefore, only three vertical wind speed patterns are required to characterize most of the gathered data. Cluster 8 and 9 represent examples of unusual shapes for vertical wind speed curves, which would need a more detailed analysis. Moreover, these profiles differ significantly from classical approaches based on a power and logarithmic laws –see eq. (1) and (2)–. An analytical function analysis is then required by these vertical wind speed profiles. It is currently a field of interest for the authors. From these results, the proposed characterization process then allows us to identify the most likely vertical wind speed patterns by considering the gathered data in a specific location and attending to the different hours. Moreover, a comparison between the vertical wind speed patterns for different hours are also available from these results. With this aim, Fig. 14 compares the most representative vertical wind speed patterns for different hours. In this case, these results include vertical wind speed patterns representing around 90% of the collected wind speed data for the different hours –percentages included in the legend–, and based on the percentages depicted in Fig. 11. As can be seen, these averaged vertical wind speed patterns differ significantly among them, and thus, a relevant loss of information –in terms of vertical wind speed profiles and wind resource estimation– would be then assumed if these patterns were reduced to only one representative wind speed curve. This is a relevant contribution of the paper, being thus required an alternative set of anaylitical functions to characterize real vertical wind speed data for different hours and locations. Under these assumptions, some extrapolation model functions are thus required to represent the collected wind speed profiles in an accurate and suitable way. This analysis is in line with the indirect method discussed in Section I. Nevertheless, it is outside the scope of the present work, but is currently one of the authors' fields of interest.

As an additional contribution of the paper, and in order to reduce significantly the data to be stored, the authors propose saving the most representative patterns for each hour. Consequently, only means, standard-deviations and the corresponding cluster from the collected vertical wind speed data are stored. From this reduced information, it is possible to estimate any vertical wind speed $v-H$ data for a specific hour of the day and location. Aiming to validate this additional proposal, Fig. 15 compares the estimated and collected wind speed $v-H$ profiles for the most representative clusters between 15:00 and 15:55 hour. This figure also includes some frequency histogram graphs of the Pearson's correlation coeficients of the estimated and observed data. These histograms can be considered as a measure of the estimation accuracy for the wind speed curves. By considering these frequency histogram graphs, the estimated $v-H$ wind speed profiles

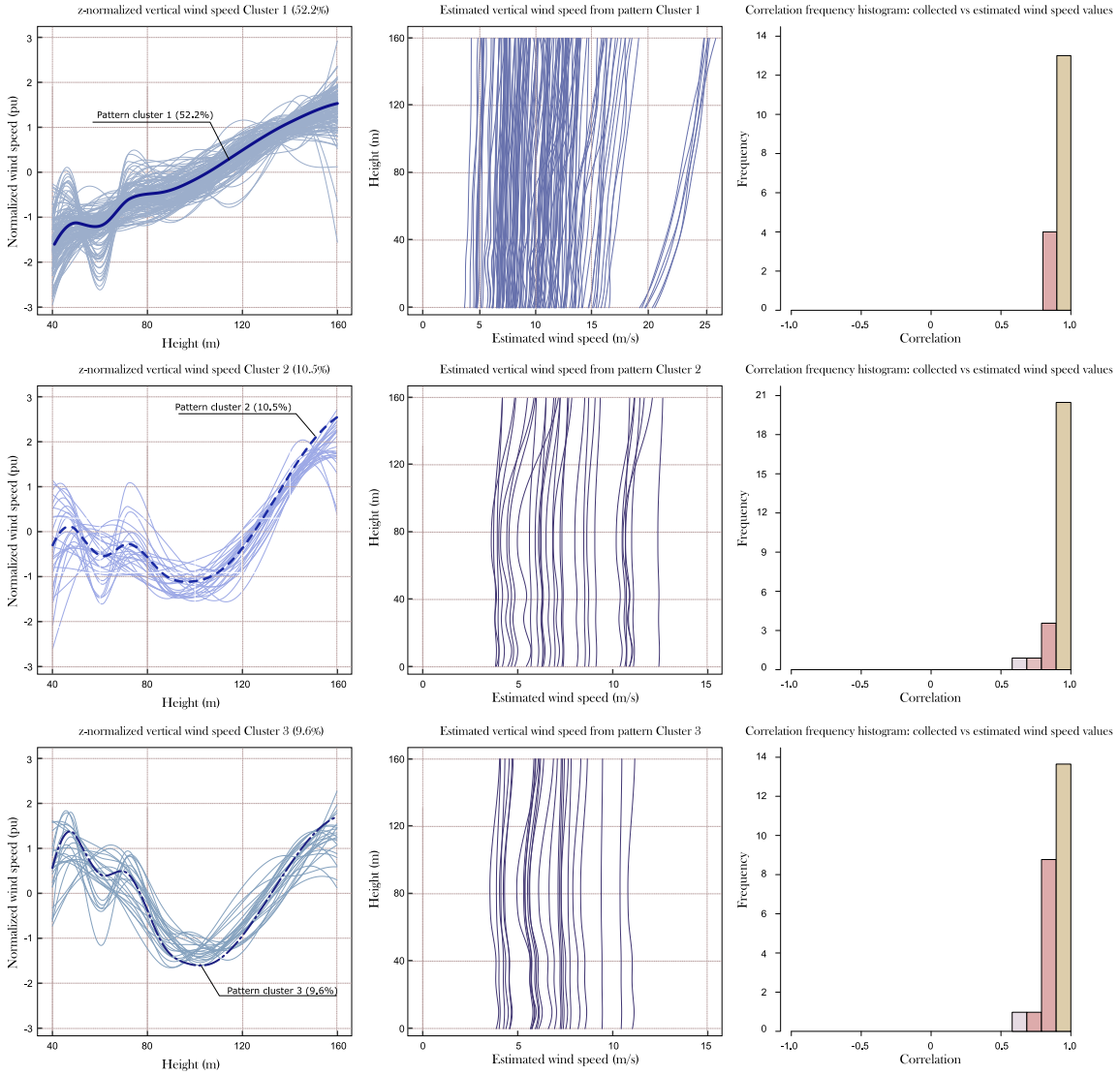

FIGURE 15. Example of estimated vs collected vertical wind speed data (Most representative clusters between 15:00 and 15:55 Hour).

are very similar to their corresponding real collected data. Therefore, the vertical wind speed clustering patterns are able to represent not only the most representative wind speed data, but also the collected $v - H$ wind speed profiles. This additional proposal allows the stored data to be significantly reduced after intensive field-test campaign measurements. Moreover, it allows a more comprehensive data structure. Each of the most representative patterns can be thus stored with their corresponding means and standard-deviation values, providing a direct estimation of the $v - H$ wind speed data.

V. CONCLUSION

A novel methodology to estimate vertical wind speed patterns from collected wind speed data is described and assessed. The proposed methodology uses a Shape-Based Distance metric to characterize wind speed similarity groups. A Ward hierarchical clustering method is applied to determine the most likely vertical wind speed patterns at each hour for a specific location. The proposed solution is assessed through real wind speed data collected with a LiDAR system over three months at a Spanish wind power plant, accounting for more than 100000 wind speed values. A preliminary filtered and homogenized process is proposed to provide scale invariance and remove inherent distortion in the initial data. From the results, at least four different vertical wind speed patterns are needed to characterize over 90% of the 6839 collected and filtered vertical wind speed profiles. Moreover, significant differences among patterns are found and subsequently, new analytical function criteria should be proposed as vertical wind speed value extrapolation models. All analyses were implemented using open-source *R*-software. The *R* code is available from the authors upon request. Further analysis of alternative extrapolation model functions to characterize in

detail the incoming wind speed at the rotor swept area is currently a relevant topic for future works.

REFERENCES

[1] S. Tselepis and J. Nikoletatos, "Renewable energy integration in power grids," IEA-ETSAP IRENA Technol., Tech. Rep., Apr. 2015. [Online]. Available: www.etsap.org–www.irena.org
[2] A. Thakur, S. Panigrahi, and R. R. Behera, "A review on wind energy conversion system and enabling technology," in *Proc. Int. Conf. Elect. Power Energy Syst. (ICEPES)*, Dec. 2016, pp. 527–532.
[3] *Wind Energy in Europe: Scenarios for 2030*, Wind Eur., Brussels, Belgium, 2017.
[4] G. J. Herbert, S. Iniyan, E. Sreevalsan, and S. Rajapandian, "A review of wind energy technologies," *Renew. Sustain. Energy Rev.*, vol. 11, no. 6, pp. 1117–1145, 2007.
[5] J. Jallad, S. Mekhilef, and H. Mokhlis, "Frequency regulation strategies in grid integrated offshore wind turbines via VSC-HVDC technology: A review," *Energies*, vol. 10, no. 9, p. 1244, 2017.
[6] S.-E. Gryning, R. Floors, A. Peña, E. Batchvarova, and B. Brümmer, "Weibull wind-speed distribution parameters derived from a combination of wind-lidar and tall-mast measurements over land, coastal and marine sites," *Boundary-Layer Meteorol.*, vol. 159, no. 2, pp. 329–348, 2016.
[7] F. Bañuelos-Ruedas, C. Angeles-Camacho, and S. Rios-Marcuello, "Analysis and validation of the methodology used in the extrapolation of wind speed data at different heights," *Renew. Sustain. Energy Rev.*, vol. 14, no. 8, pp. 2383–2391, 2010.
[8] A. Honrubia-Escribano, E. Gómez-Lázaro, Á. Molina-García, and A. Vigueras-Rodríguez, "Wind resource assessment systems: Review of new solutions based on laser technology," *Dyna*, vol. 87, no. 5, pp. 540–548, 2012.
[9] P. Doubrawa, R. J. Barthelmie, H. Wang, S. C. Pryor, and M. J. Churchfield, "Wind turbine wake characterization from temporally disjunct 3-D measurements," *Remote Sens.*, vol. 8, no. 11, p. 939, 2016.
[10] R. Bos, A. Giyanani, and W. Bierbooms, "Assessing the severity of wind gusts with lidar," *Remote Sens.*, vol. 8, no. 9, p. 758, 2016.
[11] A. Westerhellweg, B. Canadillas, A. Beeken, and T. Neumann, "One year of LiDAR measurements at FINO1-platform: Comparison and verification to met-mast data," in *Proc. 10th German Wind Energy Conf. (DEWEK)*, 2010, pp. 1–5.
[12] M. J. Post, R. L. Schwiesow, R. E. Cupp, D. A. Haugen, and J. T. Newman, "A comparison of anemometer- and lidar-sensed wind velocity data," *J. Appl. Meteorol.*, vol. 17, no. 8, pp. 1179–1181, 1978.
[13] J. Hildebrand, G. Baumgarten, J. Fiedler, and F.-J. Lübken, "Winds and temperatures of the Arctic middle atmosphere during January measured by Doppler lidar," *Atmos. Chem. Phys.*, vol. 17, no. 21, pp. 13345–13359, 2017.
[14] E. Simley, H. First, F. Haizmann, and D. Schlipf, "Optimizing Lidars for wind turbine control applications—Results from the IEA wind task 32 Workshop," *Remote Sens.*, vol. 10, no. 6, p. 863, 2018.
[15] A. Clifton *et al.*, "IEA wind task 32: Wind lidar identifying and mitigating barriers to the adoption of wind lidar," *Remote Sens.*, vol. 10, no. 3, p. 406, 2018.
[16] S. Bradley, "Aspects of the correlation between SODAR and mast instrument winds," *J. Atmos. Ocean. Technol.*, vol. 30, no. 10, pp. 2241–2247, 2013.
[17] K. S. Khan and M. Tariq, "Wind resource assessment using SODAR and meteorological mast—A case study of Pakistan," *Renew. Sustain. Energy Rev.*, vol. 81, pp. 2443–2449, Jan. 2018.
[18] S. Lang and E. McKeogh, "LIDAR and SODAR measurements of wind speed and direction in upland terrain for wind energy purposes," *Remote Sens.*, vol. 3, no. 9, pp. 1871–1901, 2011.
[19] C. B. Hasager *et al.*, "Remote sensing observation used in offshore wind energy," *IEEE J. Sel. Topics Appl. Earth Observ. Remote Sens.*, vol. 1, no. 1, pp. 67–79, Mar. 2008.
[20] Y. Liu, D. Chen, Q. Yi, and S. Li, "Wind profiles and wave spectra for potential wind farms in South China Sea. Part I: Wind speed profile model," *Energies*, vol. 10, no. 1, p. 125, 2017.
[21] G. Gualtieri and S. Secci, "Wind shear coefficients, roughness length and energy yield over coastal locations in Southern Italy," *Renew. Energy*, vol. 36, no. 3, pp. 1081–1094, 2011.
[22] S. Shimada, Y. Takeyama, T. Kogaki, T. Ohsawa, and S. Nakamura, "Investigation of the fetch effect using onshore and offshore vertical LIDAR devices," *Remote Sens.*, vol. 10, p. 1408, Sep. 2018.
[23] Q. Li, L. Zhi, and F. Hu, "Field monitoring of boundary layer wind characteristics in urban area," *Wind Struct.*, vol. 12, no. 6, p. 553, 2009.
[24] H. W. Tieleman, "Strong wind observations in the atmospheric surface layer," *J. Wind Eng. Ind. Aerodyn.*, vol. 96, no. 1, pp. 41–77, 2008.
[25] G. Gualtieri, "Wind resource extrapolating tools for modern multi-MW wind turbines: Comparison of the Deaves and Harris model vs. the power law," *J. Wind Eng. Ind. Aerodyn.*, vol. 170, pp. 107–117, Nov. 2017.
[26] Q. Li, L. Zhi, and F. Hu, "Boundary layer wind structure from observations on a 325 m tower," *J. Wind Eng. Ind. Aerodyn.*, vol. 98, no. 12, pp. 818–832, 2010.
[27] D. R. Drew, J. F. Barlow, and S. E. Lane, "Observations of wind speed profiles over greater London, UK, using a Doppler Lidar," *J. Wind Eng. Ind. Aerodyn.*, vol. 121, pp. 98–105, Oct. 2013.
[28] M. Mohandes, S. Rehman, and S. M. Rahman, "Estimation of wind speed profile using adaptive neuro-fuzzy inference system (ANFIS)," *Appl. Energy*, vol. 88, no. 11, pp. 4024–4032, 2011.
[29] Ž. Đurisić and J. Mikulović, "A model for vertical wind speed data extrapolation for improving wind resource assessment using WAsP," *Renew. Energy*, vol. 41, pp. 407–411, May 2012. [Online]. Available: http://www.sciencedirect.com/science/article/pii/S0960148111006185
[30] M. S. Islam, M. Mohandes, and S. Rehman, "Vertical extrapolation of wind speed using artificial neural network hybrid system," *Neural Comput. Appl.*, vol. 28, no. 8, pp. 2351–2361, 2017.
[31] M. Lydia, S. S. Kumar, A. I. Selvakumar, and G. E. P. Kumar, "Wind resource estimation using wind speed and power curve models," *Renew. Energy*, vol. 83, pp. 425–434, Nov. 2015.
[32] Y. C. Liu, D. Y. Chen, S. W. Li, and P. W. Chan, "Revised power-law model to estimate the vertical variations of extreme wind speeds in China coastal regions," *J. Wind Eng. Ind. Aerodyn.*, vol. 173, pp. 227–240, Feb. 2018.
[33] F. A. Hadi, "Diagnosis of the best method for wind speed extrapolation," *Int. J. Adv. Res. Elect., Electron. Instrum. Eng.*, vol. 4, no. 10, pp. 8176–8183, 2015.
[34] H. Kikumoto, R. Ooka, H. Sugawara, and J. Lim, "Observational study of power-law approximation of wind profiles within an urban boundary layer for various wind conditions," *J. Wind Eng. Ind. Aerodyn.*, vol. 164, pp. 13–21, May 2017.
[35] S. Pindado, J. Cubas, and F. Sorribes, "The cup anemometer, a fundamental meteorological instrument for the wind energy industry. Research at the IDR/UPM Institute," *Sensors*, vol. 14, pp. 21418–21452, Jun. 2014.
[36] P. Pinson and J. W. Messner, "Application of postprocessing for renewable energy," in *Statistical Postprocessing Ensemble Forecasts*, S. Vannitsem, D. S. Wilks, and J. W. Messner, Eds. Amsterdam, The Netherlands: Elsevier, 2018, ch. 9, pp. 241–266. [Online]. Available: http://www.sciencedirect.com/science/article/pii/B9780128123720000091
[37] A. T. Abolude and W. Zhou, "A comparative computational fluid dynamic study on the effects of terrain type on hub-height wind aerodynamic properties," *Energies*, vol. 12, no. 1, pp. 1–14, 2018. [Online]. Available: http://www.mdpi.com/1996-1073/12/1/83
[38] I. Arrambide, I. Zubia, and A. Madariaga, "Critical review of offshore wind turbine energy production and site potential assessment," *Electr. Power Syst. Res.*, vol. 167, pp. 39–47, Feb. 2019. [Online]. Available: http://www.sciencedirect.com/science/article/pii/S0378779618303341
[39] R. Wagner, M. Courtney, J. Gottschall, and P. Lindelöw-Marsden, "Accounting for the speed shear in wind turbine power performance measurement," *Wind Energy*, vol. 14, no. 8, pp. 993–1004, 2011.
[40] M. Elamouri, F. B. Amar, and A. Trabelsi, "Vertical characterization of the wind mode and its effect on the wind farm profitability of Sidi Daoud–Tunisia," *Energy Convers. Manage.*, vol. 52, no. 2, pp. 1539–1549, 2011. [Online]. Available: http://www.sciencedirect.com/science/article/pii/S0196890410004589
[41] G. Gualtieri and S. Secci, "Methods to extrapolate wind resource to the turbine hub height based on power law: A 1-h wind speed vs. weibull distribution extrapolation comparison," *Renew. Energy*, vol. 43, pp. 183–200, Jul. 2012. [Online]. Available: http://www.sciencedirect.com/science/article/pii/S0960148112000109
[42] E. Gómez-Lázaro *et al.*, "Probability density function characterization for aggregated large-scale wind power based on weibull mixtures," *Energies*, vol. 9, no. 2, p. 91, 2016.
[43] A. Antoniadis, X. Brossat, J. Cugliari, and J.-M. Poggi, "Clustering functional data using wavelets," *Int. J. Wavelets, Multiresolution Inf. Process.*, vol. 11, no. 1, 2013, Art. no. 1350003.
[44] T. Tarpey and K. K. Kinateder, "Clustering functional data," *J. Classification*, vol. 20, no. 1, pp. 93–114, 2003.

[45] L. Ferreira and D. B. Hitchcock, "A comparison of hierarchical methods for clustering functional data," *Commun. Statist.-Simul. Comput.*, vol. 38, no. 9, pp. 1925–1949, 2009.
[46] V. Estivill-Castro and J. Yang, "Fast and robust general purpose clustering algorithms," in *Proc. Pacific Rim Int. Conf. Artif. Intell.*, 2000, pp. 208–218.
[47] P.-N. Tan, *Introduction to Data Mining*. London, U.K.: Pearson, 2006.
[48] L. Rokach and O. Maimon, "Clustering methods," in *Data Mining and Knowledge Discovery Handbook*. Boston, MA, USA: Springer, 2005, pp. 321–352. doi: 10.1007/0-387-25465-X_15.
[49] S. Aghabozorgi, A. S. Shirkhorshidi, and T. Y. Wah, "Time-series clustering—A decade review," *Inf. Syst.*, vol. 53, pp. 16–38, Oct./Nov. 2015. [Online]. Available: http://www.sciencedirect.com/science/article/pii/S0306437915000733
[50] H. Pirim, B. Ekşioğlu, A. D. Perkins, and Ç. Yüceer, "Clustering of high throughput gene expression data," *Comput. Oper. Res.*, vol. 39, no. 12, pp. 3046–3061, 2012. [Online]. Available: http://www.sciencedirect.com/science/article/pii/S0305054812000615
[51] G. Chicco, R. Napoli, and F. Piglione, "Comparisons among clustering techniques for electricity customer classification," *IEEE Trans. Power Syst.*, vol. 21, no. 2, pp. 933–940, May 2006.
[52] A. Goia, C. May, and G. Fusai, "Functional clustering and linear regression for peak load forecasting," *Int. J. Forecasting*, vol. 26, no. 4, pp. 700–711, 2010.
[53] M. Chaouch, "Clustering-based improvement of nonparametric functional time series forecasting: Application to intra-day household-level load curves," *IEEE Trans. Smart Grid*, vol. 5, no. 1, pp. 411–419, Jan. 2014.
[54] I. P. Panapakidis, "Clustering based day-ahead and hour-ahead bus load forecasting models," *Int. J. Elect. Power Energy Syst.*, vol. 80, pp. 171–178, Sep. 2016.
[55] V. S. Kodogiannis, M. Amina, and I. Petrounias, "A clustering-based fuzzy wavelet neural network model for short-term load forecasting," *Int. J. Neural Syst.*, vol. 23, no. 5, 2013, Oct. 1350024.
[56] D. Astolfi, F. Castellani, A. Garinei, and L. Terzi, "Data mining techniques for performance analysis of onshore wind farms," *Appl. Energy*, vol. 148, pp. 220–233, Jun. 2015. [Online]. Available: http://www.sciencedirect.com/science/article/pii/S0306261915003670
[57] R. J. Gil-Garcia, J. M. Badia-Contelles, and A. Pons-Porrata, "A general framework for agglomerative hierarchical clustering algorithms," in *Proc. 18th Int. Conf. Pattern Recognit. (ICPR)*, vol. 2, Aug. 2006, pp. 569–572.
[58] A. Bouguettaya, Q. Yu, X. Liu, X. Zhou, and A. Song, "Efficient agglomerative hierarchical clustering," *Expert Syst. Appl.*, vol. 42, no. 5, pp. 2785–2797, 2015. [Online]. Available: http://www.sciencedirect.com/science/article/pii/S0957417414006150
[59] F. Murtagh and P. Legendre, "Ward's hierarchical agglomerative clustering method: Which algorithms implement ward's criterion?" *J. Classification*, vol. 31, no. 3, pp. 274–295, 2014. doi: 10.1007/s00357-014-9161-z.
[60] S. Zolhavarieh, S. Aghabozorgi, and Y. Teh, "A review of subsequence time series clustering," *Sci. World J.*, vol. 2014, Jul. 2014, Art. no. 312521.
[61] D. Berndt and J. Clifford, "Using dynamic time warping to find patterns in time series," in *Proc. KDD Workshop*, vols. 10–16, Jan. 1994, pp. 359–370.
[62] S. Xihao and Y. Miyanaga, "Dynamic time warping for speech recognition with training part to reduce the computation," in *Proc. Int. Symp. Signals, Circuits Syst. (ISSCS)*, Jul. 2013, pp. 1–4.
[63] E. Keogh and C. A. Ratanamahatana, "Exact indexing of dynamic time warping," *Knowl. Inf. Syst.*, vol. 7, no. 3, pp. 358–386, Mar. 2005. doi: 10.1007/s10115-004-0154-9.
[64] L. Rabiner and B. Juang, *Fundamentals of Speech Recognition*. Upper Saddle River, NJ, USA: Prentice-Hall, 1993.
[65] T.-C. Fu, "A review on time series data mining," *Eng. Appl. Artif. Intell.*, vol. 24, no. 1, pp. 164–181, 2011. [Online]. Available: http://www.sciencedirect.com/science/article/pii/S0952197610001727
[66] S. Chu, E. Keogh, D. Hart, and M. Pazzani, "Iterative deepening dynamic time warping for time series," in *Proc. SIAM Int. Conf. Data Mining*, 2002, pp. 195–212.
[67] C. Cassisi, P. Montalto, M. Aliotta, A. Cannata, and A. Pulvirenti, "Similarity measures and dimensionality reduction techniques for time series data mining," in *Advances in Data Mining Knowledge Discovery and Applications*, Karahoca, Ed. IntechOpen, 2012. doi: 10.5772/3349.
[68] J. Paparrizos and L. Gravano, "k-shape: Efficient and accurate clustering of time series," in *Proc. SIGMOD Conf.*, 2015, pp. 1855–1870.
[69] T. Giorgino, "Computing and visualizing dynamic time warping alignments in R: The dtw package," *J. Stat. Softw.*, vol. 31, no. 7, pp. 1–24, 2009. [Online]. Available: http://www.jstatsoft.org/v31/i07/
[70] A. Al-Jawad *et al.*, "Using multi-dimensional dynamic time warping for TUG test instrumentation with inertial sensors," in *Proc. IEEE Int. Conf. Multisensor Fusion Integr. Intell. Syst. (MFI)*, Sep. 2012, pp. 212–218.
[71] J. Barth *et al.*, "Stride segmentation during free walk movements using multi-dimensional subsequence dynamic time warping on inertial sensor data," *Sensors*, vol. 15, no. 3, pp. 6419–6440, 2015. [Online]. Available: http://www.mdpi.com/1424-8220/15/3/6419
[72] H. Kaya and Ş. Gündüz-Öğüdücü, "SAGA: A novel signal alignment method based on genetic algorithm," *Inf. Sci.*, vol. 228, pp. 113–130, Apr. 2013. [Online]. Available: http://www.sciencedirect.com/science/article/pii/S0020025512007955
[73] F. Fahiman, J. C. Bezdek, S. M. Erfani, M. Palaniswami, and C. Leckie, "Fuzzy c-Shape: A new algorithm for clustering finite time series waveforms," in *Proc. IEEE Int. Conf. Fuzzy Syst. (FUZZ-IEEE)*, Jul. 2017, pp. 1–8.
[74] R Core Team. (2018). A Language and Environment for Statistical Computing. R Foundation for Statistical Computing, Vienna, Austria. [Online]. Available: https://www.R-project.com/
[75] A. Sarda-Espinosa. (2018). *Dtwclust: Time Series Clustering With Dynamic Time Warping Distance R Package Version 5.5.1*. [Online]. Available: http://CRAN.R-project.org/package=dtwclust
[76] H. Beck and M. Kühn, "Dynamic data filtering of long-range Doppler LiDAR wind speed measurements," *Remote Sens.*, vol. 9, no. 6, p. 561, 2017. [Online]. Available: http://www.mdpi.com/2072-4292/9/6/561
[77] H. Akima and A. Gebhardt. (2016). *Akima: Interpolation of Irregularly and Regularly Spaced Data R Package Version 0.6-2*. [Online]. Available: http://CRAN.R-project.org/package=akima
[78] Y. Jung, H. Park, D.-Z. Du, and B. L. Drake, "A decision criterion for the optimal number of clusters in hierarchical clustering," *J. Global Optim.*, vol. 25, no. 1, pp. 91–111, 2003. doi: 10.1023/A:1021394316112.
[79] L. Zheng and T. Li, "Semi-supervised hierarchical clustering," in *Proc. IEEE 11th Int. Conf. Data Mining*, Dec. 2011, pp. 982–991.

ANGEL MOLINA-GARCÍA (M'07–SM'11) was born in Murcia, Spain, in 1973. He received the degree in electrical engineering from the Universidad Politécnica de Valencia, Valencia, Spain, in 1998, and the Ph.D. degree in electrical engineering from the Universidad Politécnica de Cartagena, Cartagena, Spain, in 2003, where he is currently an Associate Professor with the Department of Electrical Engineering. His research interests include wind power generation, PV power plants, energy efficiency, and demand response.

ANA FERNÁNDEZ-GUILLAMÓN received the degree in electrical engineering from the Universidad de Castilla–La Mancha, Albacete, Spain, in 2016, and the master's degree in renewable energies from the Universidad Politécnica de Cartagena, Cartagena, Spain, in 2017, where she is currently pursuing the Ph.D. degree in the Renewable Energies and Energy Efficiency Program. Her fields of interests include wind power integration, wind turbine modeling, and frequency response strategies.

EMILIO GÓMEZ-LÁZARO (SM'10) received the M.Sc. and Ph.D. degrees in electrical engineering from the Universidad Politécnica de Valencia, Valencia, Spain, in 1995 and 2000, respectively. He is currently a Full Professor with the Department of Electrical, Electronics, and Control Engineering, Castilla–La Mancha University, Albacete, Spain, where he is also the Director of the Renewable Energy Research Institute. His research interests include modeling of wind turbines and wind farms, grid codes, power system integration studies, steady-state and dynamic analysis, and maintenance of renewable energy power plants.

ANDRÉS HONRUBIA-ESCRIBANO received the degree in electrical engineering from the Polytechnic University of Madrid, Madrid, Spain, in 2008, and the Ph.D. degree in renewable energy from the Polytechnic University of Cartagena, Cartagena, Spain, in 2012. He is currently an Associate Professor with the Department of Electrical, Electronics, and Control Engineering, Castilla–La Mancha University, Albacete, Spain. Since 2008, he has been serving for several research entities, publishing more than 65 articles in journals, books and specialized conferences, and collaborating in more than 45 research and development projects. His main research interests include the integration of wind energy into power systems.

MARÍA C. BUESO received the B.Sc. and Ph.D. degrees in mathematics from the Universidad de Granada, Granada, Spain, in 1992 and 1996, respectively. She is currently an Associate Professor with the Department of Applied Mathematics and Statistics, Universidad Politécnica de Cartagena, Cartagena, Spain. Her research interests include space-temporal modeling of stochastic processes, derivation of related inference procedures and sampling strategies, and statistical analysis, modeling, and inference of physic-chemical and environmental processes.